Published online 7 June 2011 *Nucleic Acids Research, 2011, Vol. 39, No. 17* ***7477–7486***
doi:10.1093/nar/gkr457

Centromere binding specificity in assembly of the F plasmid partition complex

Flavien Pillet[1,2,3], Aurore Sanchez[4], David Lane[5], Véronique Anton Leberre[1,2,3] and Jean-Yves Bouet[4,5,*]

[1]Université de Toulouse, INSA, UPS, INP, LISBP, 135 Avenue de Rangueil, F-31077 Toulouse, France, [2]INRA, UMR792 Ingénierie des Systèmes Biologiques et des Procédés, F-31400 Toulouse, [3]CNRS, UMR5504, F-31400 Toulouse, [4]Université de Toulouse, Université Paul Sabatier, Laboratoire de Microbiologie et Génétique Moléculaires, F-31000 Toulouse and [5]Centre National de Recherche Scientifique, LMGM, F-31000 Toulouse, France

Received March 3, 2011; Revised May 17, 2011; Accepted May 18, 2011

ABSTRACT

The segregation of plasmid F of *Escherichia coli* is highly reliable. The Sop partition locus, responsible for this stable maintenance, is composed of two genes, *sopA* and *sopB* and a centromere, *sopC*, consisting of 12 direct repeats of 43 bp. Each repeat carries a 16-bp inverted repeat motif to which SopB binds to form a nucleoprotein assembly called the partition complex. A database search for sequences closely related to *sopC* revealed unexpected features that appeared highly conserved. We have investigated the requirements for specific SopB–*sopC* interactions using a surface plasmon resonance imaging technique. We show that (i) only 10 repeats interact specifically with SopB, (ii) no base outside the 16-bp *sopC* sites is involved in binding specificity, whereas five bases present in each arm are required for interactions, and (iii) the A-C central bases contribute to binding efficiency by conforming to a need for a purine–pyrimidine dinucleotide. We have refined the SopB–*sopC* binding pattern by electro-mobility shift assay and found that all 16 bp are necessary for optimal SopB binding. These data and the model we propose, define the basis of the high binding specificity of F partition complex assembly, without which, dispersal of SopB over DNA would result in defective segregation.

INTRODUCTION

Faithful inheritance of chromosomal and extra-chromosomal DNA requires specialized molecular machines in eukaryotes and most prokaryotes (1,2). For low copy number bacterial plasmids, loci ensuring active segregation to daughter cells before septum formation were identified over 30 years ago (3,4). Such partition loci are also present on most bacterial chromosomes (5). Virtually, all these loci specify three elements: a centromere, a centromere binding protein (CBP) and a NTPase. Interactions between these partners are essential for the partition process and of these, the specific recognition of centromeres by CBPs to assemble partition complexes is fundamental. CBPs act as the link between the centromere and NTPases and are thus functional equivalents of eukaryotic kinetochores. It is the partition complexes that are actively segregated by partition machinery.

The known partition loci can be classified into three types on the basis of the NTPase encoded: type I, Walker box (ParA); type II, actin-like (ParM); type III, tubulin (TubZ) (6). All types are found among plasmids, but type I is the majority and is the only type present on bacterial chromosomes (5). The most clearly understood system at the molecular level is type II, in which ATP enables the actin-like ATPase to form polymers that grow bi-directionally, moving the attached plasmids in opposite directions (7). Evidence is now accumulating that the type I segregation ATPases also polymerize in response to ATP binding and that this polymerization mediates DNA segregation (8–12). However, the molecular mechanism underlying this polymerization and how it contributes to DNA segregation by interaction with partition complexes have still to be unravelled.

Given the widespread distribution of type I partition systems and the central role of the partition complexes, it is important to define the determinants that allow the specificity of binding to centromeric sequences. Type I centromeres, generically termed *parS*, are diverse in size and organization (13). They are composed of small direct repeats, of inverted repeats (IR), or of more complex

*To whom correspondence should be addressed. Tel: (+33) 561 335 906; Fax: (+33) 561 335 886; Email: jean-yves.bouet@ibcg.biotoul.fr

The authors wish it to be known that, in their opinion, the first two authors should be regarded as joint First Authors.

sequence arrangements as in the P1 centromere (14). In the case of IR sequences, they may be organized as tandem copies or present at different locations on the replicon. Chromosomal *parS* sites consist of a 16-bp IR motif as several copies, clustered close to replication origins (15) or spread throughout the origin domain as in *Bacillus subtilis* (16). Plasmid *parS* sites are typically restricted to a single locus. CBP binding to centromeres composed of the 16-bp IR motif occur generally through a single helix-turn-helix (HTH) domain, as observed for the F plasmid centromere (17). Nevertheless, the best characterized type I partition complex assembly is that of the P1 plasmid (18–20), consisting of an atypical centromere composed of two different classes of DNA repeat. The co-crystallization of a truncated version of P1 ParB with half of *parS* reveals that ParB binds as a dimer to the two binding motifs of *parS* through both HTH and dimerization domains (21), leading to more complex interactions than expected for centromeres composed of 16-bp IR motifs. In addition to specific binding, the CBPs also show significant non-specific DNA binding capacity that allows spreading to DNA adjacent to the centromere (22–24). Higher order organization of these extended partition complexes is still poorly understood for type I partition complexes.

The type I partition locus of the 100-kb conjugative plasmid F of *Escherichia coli* is composed of the ParA homolog, SopA, the centromere binding protein, SopB and the centromere, *sopC* (Figure 1). The *sopC* is organized as an array of 12 direct repeats of 43 bp (25), (see Figure 1 and Supplementary Figure S1), each containing a 16-bp IR motif. SopB is composed of several functional domains. A 3-D structure of the dimerization and HTH DNA binding domains, present in the C-terminal part of SopB, has recently been determined by X-ray analysis and a co-crystal structure of SopB (155–323)-*sopC* was also resolved at medium resolution (17). The N-terminal part of SopB is also multifunctional, but owing to its high flexibility, its structure is unknown (17). This part contains the SopA-interaction domain (26), the arginine-finger and the putative arginine-loop motifs that stimulate SopA ATPase activity (27) and possibly a SopB dimer–dimer interaction region (28).

SopB binds to *sopC* with high affinity (29) through an HTH motif (17,26). Upon binding, it induces ~50° bend on the DNA (29), that if accumulated over the 12 *sopC* sites could organize the F partition complex into a specific structure. The co-crystal structure of SopB (155–323) with *sopC* was however intriguing in two ways: (i) each of the HTH motifs of a SopB dimer contacts only one arm of a single *sopC* and (ii) *sopC* DNA is not bent; both are in contradiction with two previous studies (28,29). Like other ParBs, SopB not only assembles specifically on its centromere but also extends the complex by spreading along the DNA on either side of *sopC* (22); it might also spread *in trans* to different DNA molecules (17). *In vivo*, SopB bound to *sopC* and flanking DNA prevents negative supercoiling of the bound DNA (29,30), suggesting that the F partition complex shields DNA from the action of other proteins.

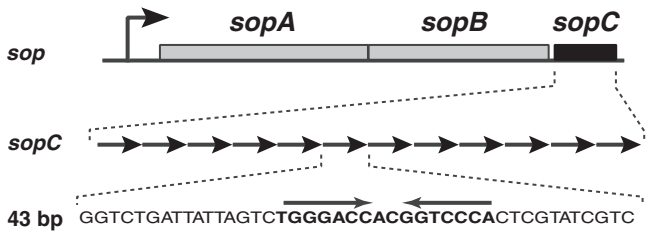

Figure 1. Organization of the F partition locus. The *sop* locus comprises two genes, *sopA* and *sopB* and a *cis*-acting centromeric site, *sopC*, composed of 12 direct repeats in tandem of 43-bp (represented by the repeated arrows). Each 43-bp unit contains a 16-bp SopB binding site. The inverted arrows indicate the SopB binding site. The bottom line shows the 43-bp consensus sequence (see Supplementary Figure S1 for the complete sequence alignment).

The role of SopB binding to DNA extends beyond that of a mere adaptor. The ATPase activity of SopA, as of ParAs generally, is very weak but is stimulated by DNA in the presence of SopB (10,31). Maximum activation is achieved when SopA interacts both with non-specific DNA and with SopB assembled on *sopC* (27). High levels of ATP hydrolysis by SopA thus occur close to assembled partition complexes. In addition, SopB has two roles on the formation of SopA filaments *in vitro*: it directly stimulates SopA polymerization and it counteracts the DNA inhibition of SopA polymerization by masking DNA in the vicinity of the centromere through the spreading/oligomerization activity (10). These roles of SopB are thought to restrict formation of SopA polymers to the place where partition complexes are assembled. Thus, SopB-mediated stimulation of SopA activities is effective where SopB molecules are concentrated, i.e. around the *sopC* nucleation point. Since SopB binds non-specific DNA, it is crucial that partition complexes are specifically assembled only on centromeric sequences. Specificity determinants involved in SopB–*sopC* interaction have not yet been determined and the bases that are required for the assembly of the F partition complex are thus not known.

The 16-bp SopB binding motif is strongly conserved and thus prevents us from deducing which bases are involved in SopB binding specificity. To identify at the nucleotide level the specific determinants needed to initiate F partition complex assembly, we first searched databases for sequences closely related to *sopC*. The sequences exhibited unexpected features. By using high-throughput surface plasmon resonance imaging (SPRi), we have characterized the DNA binding requirements for specific SopB–*sopC* interactions and have found that all bases of the *sopC* binding site are needed for maximal SopB binding strength.

MATERIALS AND METHODS

Proteins and cell extracts

SopB was purified as previously described (10,27). Crude extracts containing SopB were produced from strain DLT812 (32) carrying the SopB expression vector pDAG170 (10), as follows. LB was inoculated by 100-fold dilution of an overnight culture of strain DLT812/pDAG170 and incubated at 37°C. At OD_{600}

~0.5, SopB production was induced by adding 0.1% arabinose. At 4 h after induction, cells were harvested by centrifugation, washed in TNE (50 mM Tris–HCl, 50 mM NaCl, 1 mM EDTA), resuspended to an OD_{600} ~200 in TNE supplemented with lysozyme (500 μg ml^{-1}) and NaCl (200 mM) and left on ice for 30 min. Viscosity was then reduced by sonication and cell-free extracts were obtained by centrifugation at 4°C for 20 min at 22 000*g*. Aliquots of crude extracts were then frozen rapidly in liquid nitrogen, allowing the same SopB extract to be used for all SPRi assays reported in this study. SopB was estimated by SDS–PAGE to constitute 10–15% of crude extract protein.

SPRi assays

SPRi analysis was performed using a SPRi-Plex system from GenOptics HORIBA-scientific (France). Synthetic 65-mer oligonucleotide probes, modified at their 5′-ends with a thiol function, were obtained from Sigma and spotted on SPRi-BiochipsTM covered with a 50 nm gold film specially developed for SPRi processing (prisms from GenOptics). Spots of thiol-modified oligonucleotides (25 μM) in spotting buffer (3× SSC, 450 mM NaCl and 45 mM sodium citrate, pH 7) were applied using a ChipWriterPro contact spotter (Biorad) with solid pin SSP015 from Arrayit Corporation. At least two spots of each oligonucleotide were deposited on prisms. Before reflectivity measurement, the best angle of incidence for each sensor-chip was chosen as described (33). SPRi experiments were done in R buffer (20 mM HEPES pH 7.4, 100 mM KCl, 50 μg ml^{-1} salmon sperm DNA and 1 mM DTT) at a flow rate of 50 μl min^{-1}. Injections of target molecules (200 μl), either purified SopB or SopB-containing cell extracts diluted in R buffer, were carried out after saturation of the prism surface with Denhardt solution (Sigma). The reflectivity responses were obtained after subtraction of the averaged signal obtained on C1 probes. Reflectivity values were measured at the end of target injection (240 s), just before washing with R buffer. After each SopB interaction measurement, the surface was regenerated with NaOH 0.1 M. Data were analysed with Genoptics software SPRiAnalysis1.2.1.

Electro-mobility shift assays

Gel retardation assays were performed essentially as described (18), using 0.3 nM of annealed oligonucleotides (30 bp) 5′-^{32}P radiolabelled by polynucleotide kinase. Duplex oligonucleotides (E1, E2, E19, E23, E39, E40 and E46) were based on the *sopC* consensus: ATTAGT CtgggaccacggtcccaCTCGTAT, with upper case letters being invariant and lower case letters representing the sequence and its variations (see highlighted nucleotides in Figure 6). Binding reactions were assembled on ice in a buffer containing 30 mM HEPES–KOH (pH 7.5), 100 mM KCl, 100 μg ml^{-1} bovine serum albumin, 100 μg ml^{-1} sonicated salmon sperm DNA, 10% glycerol and 1 mM dithiothreitol and incubated 15 min at 30°C. Products were resolved at 4°C by electrophoresis on pre-run 6% polyacrylamide gels in TBE (90 mM Tris borate, 1 mM EDTA) for 150 min at 160 V. Quantification of free probes and shifted DNA complexes were quantified using MultiGauge software (Fugi). GraphPad Prism (V4.03) software was used for graphs, curve fitting and K_D calculation.

RESULTS

Centromeres related to F *sopC* are highly conserved

To define the bases required for specificity in the assembly of the partition complex on the F centromeric sequence, we used Blastn (NCBI) to search the nr nucleotide database for close homologs of F *sopC*, according to two criteria: (i) homology to the 16-bp SopB binding site, using several variations of the consensus binding site 5′-TGGGACCACGGTCCCA-3′ and (ii) at least two tandem repetitions of the sequence. This search yielded 22 different *sopC*-related centromeres that conformed to the SopB binding site, i.e. none consisted of repeats of a minor variant. Sequence alignments are presented in Supplementary Figure S3 and data are summarized in Table 1. We also found several centromeric sequences with the F SopB binding site consensus on three bacteriophage genomes. These were not repeated in tandem but dispersed over the genome and for this reason they were not included in this analysis.

All sequences recovered belong to plasmids and none to chromosomes. They are present only in bacteria of the Enterobacteriaceae, indicating that Sop subfamily of centromeric sequences is not widespread amongst bacteria. The number of tandem repeats is highly variable, from 3 in pYVe227 (*Yersinia enterocolitica*) to 17 in pKN3 (*Klebsiella pneumoniae*). While most of the *sopC* centromeric sequences (16 over 22) are composed of 43-bp repeats, as for the F archetype, one centromere has 44-bp repeat units and five have 45-bp units. In total, we therefore had 205 SopB binding sites for analysis. Only two centromeres, those of pCVM and pLVPK, are composed solely of perfect 16-bp consensus binding sites; all others include variant SopB binding sites. Most of the variations occur on the first and last repeats, especially in smaller centromeres (Table 1). Only 4 of the 22 centromeres have consensus binding sites on the terminal tandem repeats.

The high divergence of the binding sites in the first and last repeats raises doubts as to their SopB binding capacity (also see below). Hence, we excluded these repeats from further analysis. Within the remaining 161 binding sites, only 34 base variations from the consensus were observed. Fourteen of these are variants of the central A-C dinucleotide that, notably, maintain the sequence Purine–Pyrimidine (Pu–Py) (Table 1). Of the 20 remaining variants, 8 are at the third position of the consensus site and the others at any position except the seventh.

This analysis reveals the central Pu–Py and the seventh base as probable important determinants of SopB binding. The strong conservation of the others, with the exception of position three, suggests they may be as well. Clearly, targeted mutagenesis was needed to further define the bases required for SopB binding.

Table 1. Summary of sequence conservation analysis of *sopC* centromere homologs

Names (organism)	Repeats no.[a] (bp)	Consensus binding site[b]	Canonical first and last IR	Pu–Py central	Mutations at positions no.[c] 2,4,5,6,7
pKPN3 (Kp)	17 (43)	14	1	all	1
p1658 (Ec)	16 (43)	13	1	all	1
pVM01 (Ec)	13 (43)	10	1	all	1
pCVM (Se)	12 (43)	12	2	all	0
pLVPK (Kp)	12 (43)	12	2	all	0
pK2044 (Kp)	12 (43)	11	1	all	0
pSC138 (Se)	12 (43)	11	2	all	0
pAPEC-1 (Ec)	12 (43)	9	1	all	1
pColBM (Ec)	12 (43)	9	1	all	1
F (Ec)	12 (43)	8	0	all	2
pYPTS01 (Ypt)	11 (**45**)	8	0	all	1
pECOS88 (Ec)	11 (43)	8	1	all	1
pU302L (St)	10 (43)	7	0	all	1
pYV (Ypt)	8 (**45**)	6	0	all	0
pKP187 (Kp)	8 (**44**)	7	2	all	0
pVir68 (Ec)	8 (43)	6	0	all	0
pCD1 (Yp)	7 (**45**)	5	0	all	0
pYVa127 (Ye)	6 (**45**)	4	0	all	0
pO157 (Ec)	6 (43)	4	0	all	0
pCD (Yp)	5 (**45**)	3	0	all	0
pETEC74 (Ec)	4 (43)	2	0	all	0
pYVe227 (Ye)	3 (43)	0	0	all	0

Homologs of the *sopC* centromere were searched using Blastn (NCBI) and were found in bacteria closely related to *E. coli* (first column). When two or more identical *sopC* centromeres are present on different plasmids, only one is reported (see Supplementary Figure S3). The number of repeats present in each centromere of plasmids is indicated in the second column, with the length of the repeat in brackets. The numbers of perfect consensus IR SopB binding sites and of canonical first and last repeats are shown in third and fourth columns, respectively. IRs without a Pu–Py central position are numbered in the fifth column and the number of mutations compared with the consensus at positions important for SopB binding according to SPRi analysis (Numbers 2, 4, 5, 6 and 7; Figure 5) for all repeats of each centromere are shown in the last column. Ec: *E. coli*; Kp: *K. pneumoniae*; Se: *Salmonella enterica*; St: *Salmonella thyphimurium*; Ye: *Y. enterocolitica*; Yp: *Yersinia pestis*; Ypt: *Yersinia pseudotuberculosis*. pCVM, pColBM and pYVa127 are abbreviations of pCVM19633, pAPEC-ColBM and pYVa127/90, respectively.

[a]Number of repeats in each centromeric sequence with the size in nucleotides of each repeat indicated in bracket; bold values highlight differences with the standard 43-bp repeats.

[b]TGGGACC Pu–Py GGTCCCA.

[c]First and last *sopC* repeats are excluded from this calculation; positions are numbered according to Figure 5.

SPRi setup for SopB–*sopC* specific interaction analysis

We performed SPRi experiments that allow efficient screening of a large number of sequence variations. Briefly, SPRi is based on SPR technology, with the SPR signal monitored by camera, allowing simultaneous analysis of several dozen interactions in real time (34,35). Oligonucleotides with a thiol group at their 5′-ends were directly coupled to a gold sensor-chip [see 'Materials and Methods' section); (33)]. They were designed as palindromes to enable formation by self-annealing of 30-bp DNA duplexes with a single stranded hairpin at the apex (Figure 2A). Oligonucleotide C2 corresponds to the consensus SopB binding site while C1, taken as the reference (for subtracting background), has a random sequence with the same nucleotide composition as C2 (Figure 2B); (see 'Materials and Methods' section). All the SPRi data presented in the following sections come from a single sensor-chip, preliminary settings having been established on three preceding ones.

When purified SopB was injected, a specific interaction was readily detected by plotting the differential response obtained with C2 and C1 probes (Figure 2C, left). The intensity of the response curve was proportional to SopB concentration. In parallel, we also performed SPRi assays with a crude extract of cells in which SopB had been overproduced (Figure 2C, right), to test the possibility of directly assaying a protein of interest without the need for purification. The specific SopB–*sopC* interaction was readily detectable and proportional to the amount of extract, indicating that SopB-containing crude extract could be further tested along with purified SopB to provide a complete comparison of these two different SopB preparations. In both cases, we verified that SopB does not bind specifically to single strand DNA at any concentration tested (Figure 2C; dotted lines).

We were not able to calculate accurate affinity constants for SopB–*sopC* interaction, because the sensitivity of the SPRi technique is not as high as the SPR using the Biacore system, with which we had been able to measure a K_D of 2.5 nM (27). However, the response intensity at a given SopB concentration, in the 150–400 nM range, is highly reproducible (see below). We therefore used the maximum signal response obtained in the differential response curve for probes carrying sequence variations to identify the determinants for SopB binding to *sopC*. All subsequent analyses were performed with both purified SopB and SopB-containing extract.

SopB does not bind the 1st and 12th repeats of *sopC* centromere

The first and last *sopC* repeats are the most divergent, both in *sopC* and the other F-related centromeres (Table 1 and Supplementary Figure S3). We assayed their binding properties using Probes C24 and C25, corresponding to 1st and 12th *sopC* repeats of F *sopC*, respectively (Figure 3). No interaction was detected with purified SopB or with SopB-containing extract. We also tested these binding sites in their natural context (Probes C26 and C27), in fragments equivalent to the 30-bp consensus probe, but again no interaction with SopB was detected. Hence, the 1st and 12th repeats do not bind SopB efficiently *in vitro*. This result agrees with a previous DNAseI footprinting experiment which showed that the first repeat was not protected by SopB (36).

The 16-bp IR is sufficient for SopB binding specificity

DNAse I footprinting of *sopC in vitro* (36) and *in vivo* (29) indicated that SopB protected only the 16-bp IR sequences. However, the 43-bp tandem repeats of F are highly conserved, suggesting that sequences surrounding the IR might play some role in SopB binding. We tested this possibility with Probes C28 and C29, which carry three base changes immediately to the left and on both sides of the IR, respectively. SopB interaction was as efficient as with the consensus C2 in both cases (Figure 3).

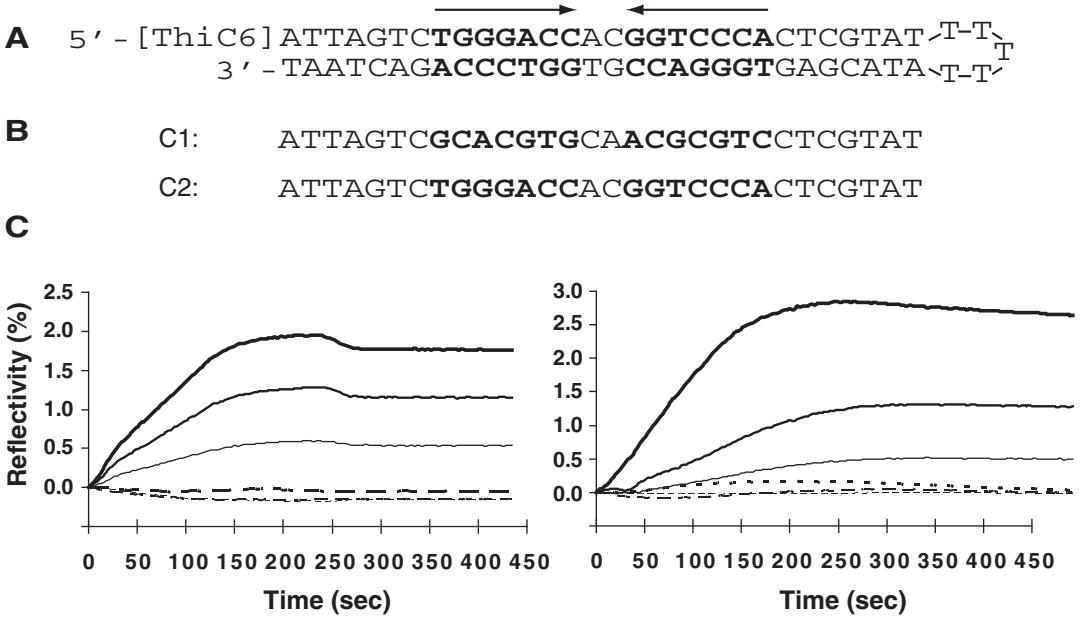

Figure 2. SPRi analysis of SopB binding to *sopC*. (**A**) Folding of the 5′ thiol-labelled 65-mer single strand oligonucleotide; the sequence of oligonucleotide C2 is shown. (**B**) Sequences of the C1 (negative control) and C2 (consensus binding site) oligonucleotides. Note that the 16-bp consensus sequence present in C2 has been shuffled to generate C1. (**C**) SPRi dose response analysis. Results, expressed as the difference in reflectivity (%) between the signals obtained with the test and non-specific C1 probes and plotted as a function of time (seconds), were generated with purified SopB (left graph) or crude extract enriched in SopB (right graph). Buffer containing purified SopB at various concentrations (50, 100 and 150 nM; thin, medium and thick lines, respectively), or various dilutions of SopB extract (1/5000, 1/2000 and 1/1000; thin, medium and thick lines, respectively) were injected at time 0, followed by washing buffer (without SopB) after 200 s (see 'Materials and Methods' section). Full lines correspond to 65-mer C2 probes adopting a double strand folding and dotted lines to 30-mer C2 probes in single strand form.

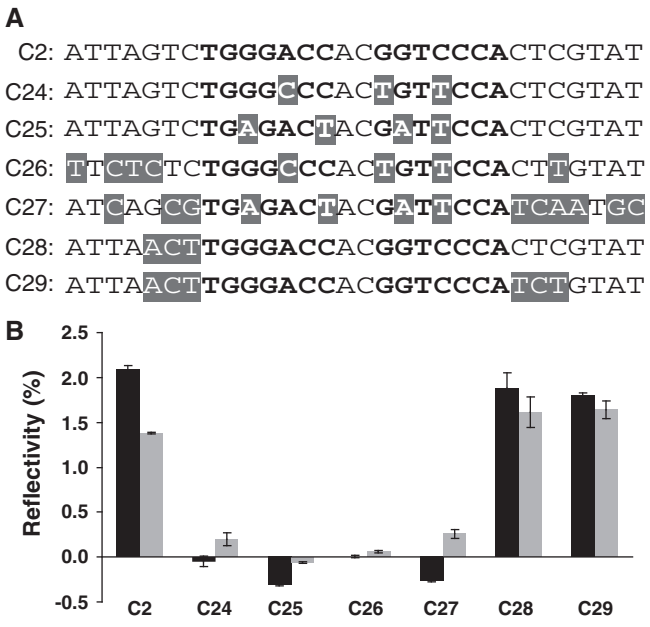

Figure 3. The 1st and 12th *sopC* repeats do not bind SopB. (**A**) Relevant sequences of analysed SPRi probes are shown below the consensus C2 probe. Left and right arms of the SopB binding site are in bold. Highlighted nucleotides indicate changes to the *sopC* consensus. (**B**) Histogram of SPRi signals for tested probes. Dark and grey bars represent the maximum of reflectivity (%) observed with purified SopB (250 nM) and with SopB-containing crude extract (1/500), respectively. Values are averages of duplicate readings on the same sensor-chip.

This result indicates that all site-specific binding determinants are present within the 16-bp IR sequence.

The central A-C is involved in SopB binding

The 16-bp IR includes a non-palindromic A-C central sequence. Only one of the twelve central dinucleotides of F *sopC* is different, A-T in the sixth IR (Supplementary Figure S1). To test whether these two central bases are important for the binding properties of SopB, as our *in silico* analysis had suggested (see above), we designed six probes with different central dinucleotides (Probes C3–C8; Figure 4). SopB interacted with Probes C3 and C7 about as strongly as with the consensus C2 probe, indicating that these modifications, C–T and A–G, do not affect binding. Notably, C3 corresponds to the naturally occurring A–T central sequence, suggesting that *in vivo,* this binding site is as efficient as the WT. All other probes tested (C4–6 and C8) showed a decrease in the SPRi signal of ~50%. This significant binding defect is found both with purified SopB and with SopB-containing cell extract. Probes C3 and C7 differ from the others in having a Pu–Py at the central position. These results, together with the observation that all the natural variations found in the central A-C conserve a Pu–Py composition (see above), imply that an important requirement for SopB binding is a Pu–Py sequence at the centre of the binding site.

To confirm the importance of Pu–Py central bases for SopB binding, we used Probe C40, which consists of a

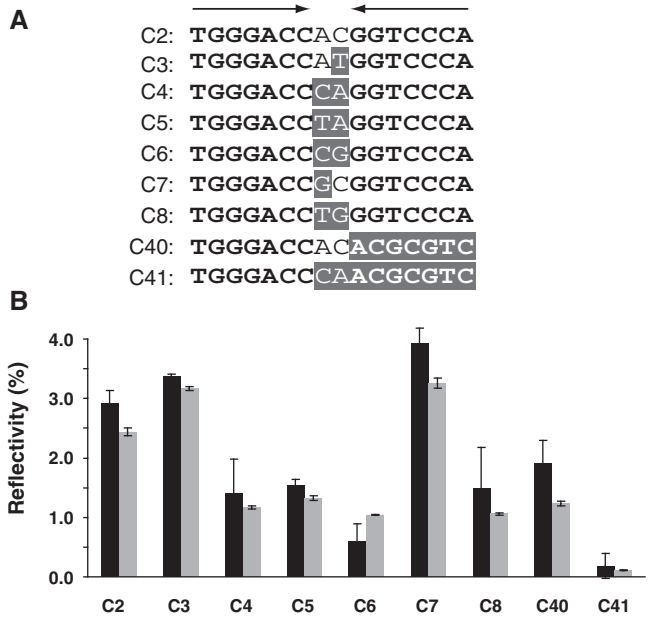

Figure 4. Non-palindromic A-C central bases are involved in SopB binding. (**A**) Sequences of analysed SPRi probes are shown below the consensus C2 probe as described in legend of Figure 3. Arrows on top represent the inverted-repeat motif. (**B**) Histogram of SPRi signals for tested probes. Dark and grey bars represent the maximum of reflectivity (%) observed with purified SopB (400 nM) or with SopB-containing crude extract (1/200), respectively. Values are averages of duplicate readings on the same sensor-chip.

half-binding site with the central A-C; the right arm being randomized as for Probe C1 (Figure 4). SPRi measurements indicated that C40 bound SopB less strongly (~50% of SPRi signal compared to C2). The equivalent probe with the central A-C changed to C-A (Py–Pu; Probe C41) showed no detectable interaction with either purified SopB or SopB-containing cell extract (Figure 4). Thus, combining removal of one arm with conversion of the central dyad to Py–Pu prevents stable complex formation, indicating that the changes are cumulative. These results clearly demonstrate that the Pu–Py central bases are necessary for fully efficient binding of SopB to the 16-bp IR motif.

Base pairs in *sopC* arms involved in SopB–*sopC* interaction specificity

To determine which bases in right and left arms of the 16-bp IR motif are involved in the specificity of binding, we made single base changes at each position or symmetrical base changes in both arms (positions are noted as 1–7; see Figure 5A). As shown above, removing a complete arm reduces to ~50% the SPRi signal obtained with SopB (Probe C40, Figure 4). Therefore, SPRi signals with probes carrying single changes are expected to be between 50% and 100% of that obtained with the consensus probe (C2). Indeed, we found this to be the case for all single base changes (Figure 5B).

Variations at Position 1 gave no significant reduction in SopB binding intensity when either single (C22) or double changes (C23) are made. Similar changes at Position 3 (C18 and C19) gave only minor reductions. Positions 1 and 3 thus appear to be unimportant for SopB binding specificity in this assay. By contrast, SopB interactions are significantly affected by single changes at Positions 2, 4, 5, 6 and 7 (Figure 5).

At two Positions (2 and 7) the reduction in signal depended on which arm carried the base change (Figure 5, compare C14–C145 and C20–C205). However, when changes were made on both arms for these two Positions (C15 and C21), SPRi signals were barely detectable, indicating that these positions are needed for SopB binding. At Position 4, symmetrical change (C11) resulted in an ~80% decrease in the SPRi intensity with both SopB and SopB-containing cell extract, indicating that this position is involved but not as strongly as Positions 2, 5–7. A discrepancy was observed with Probe C13, which retained ~20% of SPRi signal with purified SopB but was completely deficient when SopB-containing extract was used. This difference was not observed on a previous sensor-chip (no interaction was detected; data not shown), confirming that the double change on Position 6 abolished SopB interaction. These data indicate that the five Positions (2, 4, 5, 6 and 7) are important for SopB binding *in vitro*.

We also tested several combinations of multiple changes on one arm (Figure 5; Probes C42–C44). They all showed the same binding deficiency (~50% reduction in the SPRi signal) as observed when only one arm is present (Figure 4, Probe C40) and bound significantly better than a probe (C45) with variations in both arms.

It is interesting to note that amongst all the closely related *sopC* centromeres that have fewer than ten repeats, variations relative to the consensus are found exclusively on Positions 1 and 3 (Table 1 and Supplementary Figure S3; variations on first and last repeats are not considered). In addition, none of the three repeats present on the smallest centromere (pYVe227) have a consensus SopB binding site. However, variations on both the first and second repeats are restricted to Positions 1 and 3. These natural variations thus reinforce the results of the SPRi analysis in suggesting that Positions 2, 4, 5, 6 and 7 are the most important for SopB–*sopC* binding specificity.

Definition of the minimal SopB binding site

To confirm the binding specificity pattern observed in SPRi analysis, we performed electro-mobility shift assays (EMSA), which allow accurate measurement of SopB binding constants. DNA duplexes of 30 bp carrying the consensus or variant binding sites (see 'Materials and Methods' section) were incubated with increasing concentrations of SopB and subjected to EMSA analysis (Supplementary Figure S2) and binding curves were generated (Figure 6). About 50% of the *sopC* consensus probe (E2) was shifted at 3 nM of SopB (Figure 6, bottom), while no disappearance of the free probe carrying a shuffled sequence of the same nucleotide composition was observed (Probe E1; Supplementary Figure S2). Affinity constants (K_D) were estimated after fitting binding curves to a one-site binding hyperbola equation. SopB binds to the consensus 16-bp IR on the 30-bp probe with a K_D of

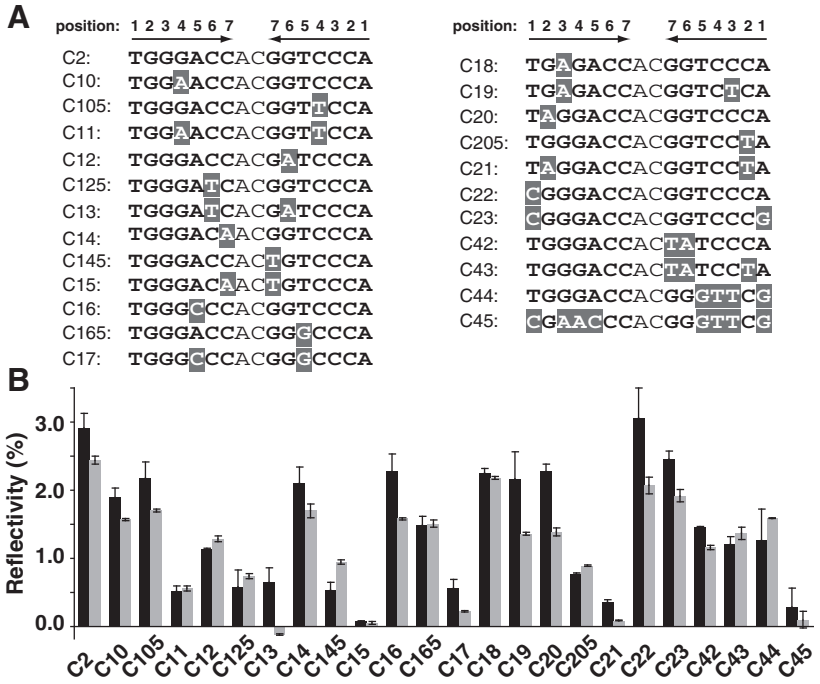

Figure 5. Five bases in each arm are required for efficient binding. (**A**) Sequences of analysed SPRi probes are shown below the consensus C2 probe as described in legend of Figure 3. Positions in both arms are numbered symmetrically from 1 to 7 due to their palindromic nature. (**B**) Histogram of SPRi signals for tested probes. Dark and grey bars represent the maximum of reflectivity (%) observed with purified SopB (400 nM) or with SopB-containing crude extract (1/200), respectively. Values are average of duplicate readings on the same sensor-chip.

2.6 nM, similar to values determined previously with longer DNA fragments containing a 43-bp repeat (27). No interaction was detected between SopB and Probe E45, equivalent to the SPRi Probe C45 (data not shown) or with Probe E46 carrying three variations on both arms at Positions 1, 3 and 4 (Supplementary Figure S2). When only two variations were present at Positions 1 and 3 on both arms (Probe E39), interaction with SopB was detected but binding affinity was decreased 15-fold (K_D = 40 nM; Figure 6). This loss of DNA binding efficiency was higher than expected from the SPRi data, which showed that individually these two variations did not significantly reduce SopB binding. We therefore measured binding affinities of *sopC* probes containing variations on both arms at Positions 1 (E23) or 3 (E19) and found SopB binding deficiencies of about 2.5- and 7-fold, respectively (Figure 6 and Supplementary Figure S2). These results are compatible with the SPRi measurements and indicate that binding deficiencies at Positions 1 and 3 are cumulative.

Model for SopB–*sopC* interaction

Our SPRi and EMSA assays measured only the specific binding of SopB to *sopC*. They were performed in the presence of non-specific DNA as competitor and in the case of SPRi analysis the binding curve was the differential response between signals obtained with tested and reference probes. We found that (i) five of seven bases in both arms of *sopC* are strongly involved in the specificity of SopB binding (Figure 5), (ii) bases at Positions 1 and 3 are required for optimal SopB binding (Figure 6) and (iii) Pu–Py central bases contribute to efficient SopB–*sopC* interaction (Figure 4), revealing that all 16 bp in *sopC* site are involved in specific binding. A clear picture of the bases involved in specific binding of SopB to *sopC* can thus be generated (Figure 7).

Recently, the co-crystal structure of a SopB–*sopC* complex was resolved at about 3.5 Å (17), enabling prediction of likely contacts between *sopC* and positively charged amino acids present inside (R190, R191 and R195) and outside (R219) the HTH motif of SopB. Guanines at Positions 6 and 7, located close to amino acids R195 and R219, respectively, were found to be essential for binding in our SPRi analysis, strengthening the conclusion that interactions G6–R195 and G7–R219 are involved in SopB–*sopC* binding specificity. However, the degree of resolution was too low to allow distinction between guanines G2 or G3 as the base in contact with the R190 residue. Our data enable this discrimination; mutation of G2 but not of G3 strongly reduces SopB binding, indicating that R190 interacts with the former. In the case of the K191 residue, a contact with either G4 or T5, or both was suggested by Schumacher *et al.* (17). Our results, indicating that variations on both positions have similar effects, are in agreement with K191 interacting with both G4 and T5 bases. These four positively charged residues of SopB are thus the main determinants of specificity for interaction with *sopC*. They are all conserved in the cognate SopB proteins corresponding to the *sopC* sequences listed in Supplementary Figure S3, as shown in Supplementary Figure S4. No contact was found in the SopB–*sopC* structure within the Pu–Py

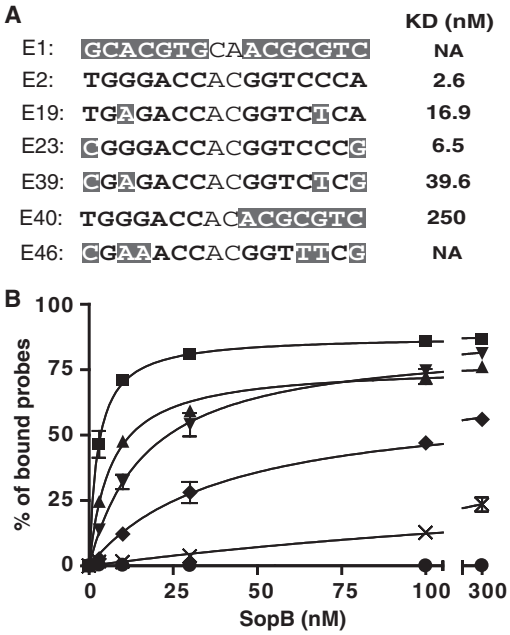

Figure 6. SopB–*sopC* binding efficiency measured by EMSA. The 30-bp DNA duplexes carrying *sopC* or variant binding sites were incubated with increasing concentrations of SopB and subjected to EMSA (see Supplementary Figure S2). (**A**) Relevant sequences of analysed probes with highlighted nucleotides indicating changes to the *sopC* consensus (Probe E2). Binding constants (K_D) for variant *sopC* sites are calculated from the fitted binding curves according to the one site binding hyperbola equation $Y = B_{max}*X/(K_d + X)$. B_{max} is the maximum binding and K_d is the concentration of ligand required to reach half-maximal binding. (**B**) Quantification after EMSA of SopB binding to Probes E1, filled circles; E2, filled square; E19, filled inverted triangle; E23, filled triangle; E39, filled diamond; E40, cross. Each data point is the average of two independent experiments except for Probe E2 which was done four times. Binding curves are fitted to the above equation with $R^2 > 0.97$.

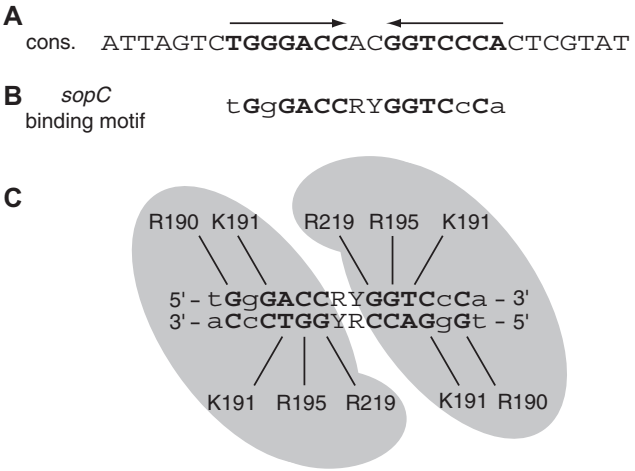

Figure 7. Refined *sopC* binding motif and model for SopB–*sopC* interactions. (**A**) The consensus sequence (cons.) of the *sopC* repeat. Arrows indicate the inverted repeat motif (bold nucleotides). (**B**) The SopB binding motif as defined by SPRi analysis. Essential nucleotides for SopB binding specificity are in bold upper case letters, important nucleotides are in upper case and nucleotides not strongly involved in specificity are in lower case. R and Y stand for purine and pyrimidine nucleotides, respectively. (**C**) Predicted interactions between amino-acids of SopB with *sopC* nucleotides. Grey zones represent the subunits of a SopB dimer. R190, R219, R195 and K191 correspond to arginines 190, 195, 219 and lysine 191. Straight lines represent suggested amino acid–nucleotide interactions.

central position, suggesting that these two bases play a role in SopB–*sopC* interaction other than direct amino acid contact.

DISCUSSION

Assembly of partition complexes is the first step of the segregation process for bacterial replicons. As it is based on selective recognition of the centromere by the binding protein, knowledge of the determinants of this specificity is necessary for understanding partition at the molecular level. Using a large scale SPRi technique in parallel with EMSA, we have identified the DNA determinants of specificity in assembly of the partition complex on the F centromere. We have shown that the specificity determinants are restricted to the 16-bp IR and that all these bases are involved, to different extents, in the binding specificity to SopB (Figure 7). Our results point to an important constraint that prevents SopB binding at wrong positions. Such mis-assembly would lead to a segregation defect due to centromere incompatibility (37,38). In the course of this study on SopB–*sopC* interaction, we also demonstrated that crude extracts containing a protein of interest could be used in the high-throughput SPRi assay, as it proved to be as sensitive as highly purified protein in detecting DNA probes (Figures 2–5). Avoiding the need to purify proteins should be useful when the aim is to test binding of protein homologs or variants to numerous probes.

The number of *sopC* repeats in the Sop subfamily of partition system is highly variable, from 3 to 17 (Table 1), indicating that the actual number of repeats is not an important feature of the centromere. Indeed, it has been shown that a single repeat is sufficient to allow the formation of a highly structured nucleoprotein complex and to ensure stability of a mini-F (39,40). The ability of SopB dimers to spread on both sides of the centromeric DNA allows the formation of an extended partition complex (22,41). Spreading beyond the centromeric DNA may thus compensate for the variability in the number of *sopC* repeats by allowing the formation of partition complexes of a size compatible with efficient partition. It may be essential in the case of smaller centromeric sites found on some plasmids (Table 1). This could also be of particular importance in the case of chromosomal *parS* centromeric sites, which also consist of 16-bp IR but are scattered throughout in the origin region or clustered near the replication origin (15,16) rather than organized as tandem repeats as in *sopC* or other plasmid centromeric sites. Spreading of the centromere binding protein is indeed a property shared by centromere binding proteins encoded on chromosomes (15,23,42).

In vitro, the 1st and 12th *sopC* repeats do not bind specifically to SopB (Figure 3), due to variations on both arms at positions important for binding. This observation

is consistent with the bulk of the analysis (Figure 5) in showing that reducing binding on both arms completely prevents SopB binding. Only 4 of the 22 centromeres have consensus binding sites in their terminal repeats (Table 1) and centromeres with fewer than 11 repeats do not have a consensus binding site on either of these repeats, with one exception (pKP187). *In vivo*, these terminal repeats should not be bound directly by SopB. However, the interaction between SopB dimers that leads to spreading might enable the docking of SopB at the normal position on these defective sites. It will be of interest to determine whether the first and last *sopC* repeats of F are efficiently bound *in vivo* and whether the pattern of DNAseI protection is similar to that on the other repeats.

The SPRi analysis revealed the importance of the non-palindromic A-C central bases in SopB binding to *sopC* and showed that the important requirement is the presence of a Pu–Py dinucleotide at these positions (Figure 4). Strikingly, all 205 SopB binding sites recovered from the database harbour a Pu–Py at the central position, even in the less conserved first and last repeats (Table 1 and Supplementary Figure S3), pointing to a key role of these two bases in SopB binding for all centromeres related to the Sop sub-family. However, in the recently published structure of SopB–*sopC* complexes (17), no residue of SopB appears to be close enough to these central bases for direct interaction. These co-crystal SopB–*sopC* structures were obtained in conditions allowing SopB dimer to bind two different DNA molecules (17), which is in disagreement with an earlier study based on use of a chimeric SopB which suggested that the SopB dimer binds to a single *sopC* site (28). Our data support the latter view in which each of the HTH motifs of a SopB dimer contacts one arm of a single *sopC* site (Figure 7). Our arguments are based on the observation that several single mutations in one arm strongly destabilize the SopB–*sopC* interaction observed in SPRi (Figure 5), reducing the binding constant (measured by EMSA; Figure 6) by 100-fold. If only one arm was engaged in the primary interaction, we would not expect such a drastic decrease in binding efficiency. Moreover, when the A-C central bases were switched to Py–Pu in a configuration with only one arm, we observed complete loss of binding (Figure 3), indicating that SopB binding to only one arm of the site is not the actual binding mode.

We previously measured a bending angle of $\sim 50^\circ$ introduced upon SopB binding to a single *sopC* repeat (29). This bending, not observed in the SopB–*sopC* structure of Schumacher *et al.* (17), would be expected to involve the binding of both HTH motifs of a SopB dimer and might also be important in the specificity of the interaction. In a model in which both HTH motifs of a dimer bound to a single *sopC* site, SopB may thus interact directly with the central Pu–Py bases. Another likely possibility is that these bases may impose a structural constraint on *sopC* DNA. The bases flanking the central ones make a Py–Pu–Py–Pu sequence arrangement in almost all sequences analysed (Supplementary Figure S3). Interestingly, it was observed that successive base planes in pyrimidine–purine steps open the angle between them (43,44). This could allow an optimal positioning of the bases present in the major groove involved in SopB interactions as well as establishing the bend.

Centromeres of the Sop sub-family are composed of variable numbers of repeats organized in direct tandem. Most SopB binding sites are precisely spaced in a 43-bp motif of relatively well conserved sequences as for plasmid F (Supplementary Figure S3). We found some exceptions—one centromere with 44-bp repeats and five with a 45-bp repeat arrangement (Table 1). Such organization with a precise spacing argues for an important role of the sequence between the 16-bp IR sites. However, our data clearly show that no base outside the *sopC* site is involved in the primary interaction with SopB (Figure 3). This suggests that the role of the regular spacing is rather in the global organization of the partition complex. The 43-bp spacing corresponds almost exactly to four helical turns of the DNA. Each *sopC* binding site is thus present on the same side of the DNA allowing each SopB dimer to be positioned regularly on the same face. In addition, the $\sim 50^\circ$ bending induced by each SopB bound to *sopC* could organize the F partition complex into a continuous protein super-helical array, wrapping the DNA about its positive convex surface to form a solenoid-shaped structure reminiscent of that observed for the type II partition complex (6). We suggest that a widespread complex architecture formed by different classes of Par system may reflect some maximally efficient configuration for interaction with partition NTPases. In order to understand the global architecture of the Sop partition complex it will be of interest to investigate more carefully the role of this regular spacing in the partition complex assembly both *in vivo* and *in vitro*.

SUPPLEMENTARY DATA

Supplementary Data are available at NAR Online.

ACKNOWLEDGEMENTS

We thank J. Rech for technical assistance, Franck Pasta and Yoan Ah-Seng for discussions and Franck Pasta and François Cornet for critical reading of the manuscript.

FUNDING

l'Agence National pour la Recherche (2010 BLAN 1316 01 to J.-Y.B., 2006 BLAN 0280 01 to D.L.); la Région Midi-Pyrénées (07005583 to V.L.); GenOptics Horiba Scientific (to F.P.); MERNT fellowship (to A.S.). Funding for open access charge: Agence National pour la Recherche N° 2010 BLAN 1316 01.

Conflict of interest statement. None declared.

REFERENCES

1. Hayes,F. and Barilla,D. (2006) The bacterial segrosome: a dynamic nucleoprotein machine for DNA trafficking and segregation. *Nat. Rev. Microbiol.*, **4**, 133–143.
2. Cheeseman,I.M. and Desai,A. (2008) Molecular architecture of the kinetochore-microtubule interface. *Nat. Rev.*, **9**, 33–46.

3. Ogura,T. and Hiraga,S. (1983) Partition mechanism of F plasmid: two plasmid gene-encoded products and a *cis*-acting region are involved in partition. *Cell*, **32**, 351–360.
4. Austin,S. and Abeles,A. (1983) Partition of unit-copy miniplasmids to daughter cells. I. P1 and F miniplasmids contain discrete, interchangeable sequences sufficient to promote equipartition. *J. Mol. Biol.*, **169**, 353–372.
5. Gerdes,K., Moller-Jensen,J. and Bugge Jensen,R. (2000) Plasmid and chromosome partitioning: surprises from phylogeny. *Mol. Microbiol.*, **37**, 455–466.
6. Schumacher,M.A., Glover,T.C., Brzoska,A.J., Jensen,S.O., Dunham,T.D., Skurray,R.A. and Firth,N. (2007) Segrosome structure revealed by a complex of ParR with centromere DNA. *Nature*, **450**, 1268–1271.
7. Garner,E.C., Campbell,C.S., Weibel,D.B. and Mullins,R.D. (2007) Reconstitution of DNA segregation driven by assembly of a prokaryotic actin homolog. *Science*, **315**, 1270–1274.
8. Barilla,D., Rosenberg,M.F., Nobbmann,U. and Hayes,F. (2005) Bacterial DNA segregation dynamics mediated by the polymerizing protein ParF. *EMBO J.*, **24**, 1453–1464.
9. Lim,G.E., Derman,A.I. and Pogliano,J. (2005) Bacterial DNA segregation by dynamic SopA polymers. *Proc. Natl Acad. Sci. USA*, **102**, 17658–17663.
10. Bouet,J.Y., Ah-Seng,Y., Benmeradi,N. and Lane,D. (2007) Polymerization of SopA partition ATPase: regulation by DNA binding and SopB. *Mol. Microbiol.*, **63**, 468–481.
11. Pratto,F., Cicek,A., Weihofen,W.A., Lurz,R., Saenger,W. and Alonso,J.C. (2008) Streptococcus pyogenes pSM19035 requires dynamic assembly of ATP-bound ParA and ParB on parS DNA during plasmid segregation. *Nucleic Acids Res.*, **36**, 3676–3689.
12. Ptacin,J.L., Lee,S.F., Garner,E.C., Toro,E., Eckart,M., Comolli,L.R., Moerner,W.E. and Shapiro,L. (2010) A spindle-like apparatus guides bacterial chromosome segregation. *Nat. Cell Biol.*, **12**, 791–798.
13. Ebersbach,G. and Gerdes,K. (2005) Plasmid segregation mechanisms. *Annu. Rev. Genet.*, **39**, 453–479.
14. Funnell,B.E. and Gagnier,L. (1993) The P1 plasmid partition complex at parS: II. Analysis of ParB protein binding activity and specificity. *J. Biol. Chem.*, **268**, 3616–3624.
15. Bartosik,A.A. and Jagura-Burdzy,G. (2005) Bacterial chromosome segregation. *Acta. Biochim. Pol.*, **52**, 1–34.
16. Lin,D.C.H. and Grossman,A.D. (1998) Identification and characterization of a bacterial chromosome partitioning site. *Cell*, **92**, 675–685.
17. Schumacher,M.A., Piro,K.M. and Xu,W. (2010) Insight into F plasmid DNA segregation revealed by structures of SopB and SopB-DNA complexes. *Nucleic Acids Res.*, **38**, 4514–4526.
18. Bouet,J.Y., Surtees,J.A. and Funnell,B.E. (2000) Stoichiometry of P1 plasmid partition complexes. *J. Biol. Chem.*, **275**, 8213–8219.
19. Schumacher,M.A., Mansoor,A. and Funnell,B.E. (2007) Structure of a four-way bridged ParB-DNA complex provides insight into P1 segrosome assembly. *J. Biol. Chem.*, **282**, 10456–10464.
20. Surtees,J.A. and Funnell,B.E. (2001) The DNA binding domains of P1 ParB and the architecture of the P1 plasmid partition complex. *J. Biol. Chem.*, **276**, 12385–12394.
21. Schumacher,M.A. and Funnell,B.E. (2005) Structures of ParB bound to DNA reveal mechanism of partition complex formation. *Nature*, **438**, 516–519.
22. Lynch,A.S. and Wang,J.C. (1995) SopB protein-meditated silencing of genes linked to the *sopC* locus of *Escherichia coli* F plasmid. *Proc. Natl Acad. Sci. USA*, **92**, 1896–1900.
23. Murray,H., Ferreira,H. and Errington,J. (2006) The bacterial chromosome segregation protein Spo0J spreads along DNA from parS nucleation sites. *Mol. Microbiol.*, **61**, 1352–1361.
24. Rodionov,O., Lobocka,M. and Yarmolinsky,M. (1999) Silencing of genes flanking the P1 plasmid centromere. *Science*, **283**, 546–549.
25. Helsberg,M. and Eichenlaub,R. (1986) Twelve 43-base-pair repeats map in a *cis*-acting region essential for partition of plasmid mini-F. *J. Bacteriol.*, **165**, 1043–1045.
26. Ravin,N.V., Rech,J. and Lane,D. (2003) Mapping of functional domains in F plasmid partition proteins reveals a bipartite SopB-recognition domain in SopA. *J. Mol. Biol.*, **329**, 875–889.
27. Ah-Seng,Y., Lopez,F., Pasta,F., Lane,D. and Bouet,J.Y. (2009) Dual role of DNA in regulating ATP hydrolysis by the SopA partition protein. *J. Biol. Chem.*, **284**, 30067–30075.
28. Hanai,R., Liu,R.P., Benedetti,P., Caron,P.R., Lynch,A.S. and Wang,J.C. (1996) Molecular dissection of a protein SopB essential for Escherichia coli F plasmid partition. *J. Biol. Chem.*, **271**, 17469–17475.
29. Bouet,J.Y. and Lane,D. (2009) Molecular basis of the supercoil deficit induced by the mini-F plasmid partition complex. *J. Biol. Chem.*, **284**, 165–173.
30. Lynch,A.S. and Wang,J.C. (1994) Use of an inducible site-specific recombinase to probe the structure of protein-DNA complexes involved in F plasmid partition in *Escherichia coli*. *J. Mol. Biol.*, **236**, 679–684.
31. Watanabe,E., Wachi,M., Yamasaki,M. and Nagai,K. (1992) ATPase activity of SopA, a protein essential for active partitioning of F-plasmid. *Mol. Gen. Genet.*, **234**, 346–352.
32. Bouet,J.Y., Bouvier,M. and Lane,D. (2006) Concerted action of plasmid maintenance functions: partition complexes create a requirement for dimer resolution. *Mol. Microbiol.*, **62**, 1447–1459.
33. Pillet,F., Thilbault,C., Bellon,S., Maillart,E., Trévisiol,E., Vieu,C., François,J.M. and Anton-Leberre,V. (2010) Simple surface chemistry to immobilize DNA probes that significantly increases sensitivity and spots density of surface plasmon resonance imaging based microarray systems. *Sensors and Actuators B*, **147**, 87–92.
34. Scarano,S., Scuffi,C., Mascini,M. and Minunni,M. (2010) Surface plasmon resonance imaging (SPRi)-based sensing: a new approach in signal sampling and management. *Biosens. Bioelectron.*, **26**, 1380–1385.
35. Maillart,E., Brengel-Pesce,K., Capela,D., Roget,A., Livache,T., Canva,M., Levy,Y. and Soussi,T. (2004) Versatile analysis of multiple macromolecular interactions by SPR imaging: application to p53 and DNA interaction. *Oncogene*, **23**, 5543–5550.
36. Mori,H., Mori,Y., Ichinose,C., Niki,H., Ogura,T., Kato,A. and Hiraga,S. (1989) Purification and characterization of SopA and SopB proteins essential for F plasmid partitioning. *J. Biol. Chem.*, **264**, 15535–15541.
37. Bouet,J.Y., Rech,J., Egloff,S., Biek,D.P. and Lane,D. (2005) Probing plasmid partition with centromere-based incompatibility. *Mol. Microbiol.*, **55**, 511–525.
38. Bouet,J.Y., Nordstrom,K. and Lane,D. (2007) Plasmid partition and incompatibility - the focus shifts. *Mol. Microbiol.*, **65**, 1405–1414.
39. Biek,D.P. and Shi,J.P. (1994) A single 43-bp sopC repeat of plasmid mini-F is sufficient to allow assembly of a functional nucleoprotein partition complex. *Proc. Natl Acad. Sci. USA*, **91**, 8027–8031.
40. Lane,D., Rothenbuehler,R., Merrillat,A. and Aiken,C. (1987) Analysis of the F plasmid centromere. *Mol. Gen. Genet.*, **207**, 406–412.
41. Biek,D.P. and Strings,J. (1995) Partition functions of mini-F affect plasmid DNA topology in *Escherichia coli*. *J. Mol. Biol.*, **246**, 388–400.
42. Breier,A.M. and Grossman,A.D. (2007) Whole-genome analysis of the chromosome partitioning and sporulation protein Spo0J (ParB) reveals spreading and origin-distal sites on the Bacillus subtilis chromosome. *Mol. Microbiol.*, **64**, 703–718.
43. Dickerson,R.E. and Drew,H.R. (1981) Kinematic model for B-DNA. *Proc. Natl Acad. Sci. USA*, **78**, 7318–7322.
44. Zhurkin,V.B. (1983) Specific alignment of nucleosomes on DNA correlates with periodic distribution of purine-pyrimidine and pyrimidine-purine dimers. *FEBS Lett.*, **158**, 293–297.